International Journal of Electronics & Informatics

ORIGINAL ARTICLE

Analysis of Silver and Gold Nanowires to Determine the Effect of Diameter Change on Cross-Sections and Local Electric Field Intensity

A. B. M Hasan Talukder[1], Md. Omar Faruk[2], and Shahida Rafique[3]*

ISSN: 2186-0114

http://www.cennser.org/IJEI

ARTICLE HISTORY

Received: 8 November, 2013
Accepted: 9 July, 2014

Published online: 16 July, 2014

Vol. 3, No. 1

Abstract

Finite Difference Time Domain analysis of metallic nanowires has been performed to determine the effect of diameter change on absorption and *scattering cross-sections and on local electric field intensity. Silver and Gold nanowires have been selected for the analysis. It has been found that, for Silver nanowire of radius 35 nm, the absorption cross-section shows a peak value of about 138 nm at around 342 nm wavelength and scattering cross-section shows a peak of about 173 nm at 352 nm wavelength whereas for Gold nanowire there exists no sharp peak in any cross-section. Similar analysis has been performed for radii of 28 nm, 27 nm, 26 nm, 25 nm, 24 nm, 20 nm and 15 nm, and it has been realized that the reduction in the radius of Silver nanowire causes negligible shift in wavelength at which the absorption cross-section peak occurs while the peak for scattering cross-section shifts to lower wavelength and also reduces the scattering cross-section to values lower than the absorption cross-section. It has also been found from the local electric field intensity distribution for different radii that Gold nanowires exhibit better resonance at lower dimension than Silver nanowires.*

Keywords: *Metallic nanowire, FDTD analysis, Cross-sections, Surface Plasmon Resonance, Local electric-field intensity*

I. INTRODUCTION

1-dimensionalnanostructures, known as Nanowires, have become the forefront of today's study on solid-state devices and technologies. With so many unique and interesting physical, optical and other properties, these nanowire structures are increasingly being considered as fundamental building blocks for the realization of entirely new classes of nanoscale devices and circuits, with applications stretching from photonics to nanoelectronics, and also from sensors to photovoltaics.

However, advancing towards the nanoscale involves the introduction and consideration of many critical phenomena and characteristic parameters. At the nanoscale, most phenomena are dominated by quantum physics and they exhibit unique behavior based on such characteristic parameters. In order to achieve minimum device sizes and ultra-high levels of integration, it is necessary to identify these critical parameters for improved performance.

AUTHORS INFO

Author 1 A.B.M Hasan Talukder*
e-mail: hasan.apece06@gmail.com
Address: Dept. of Applied Physics, Electronics & Communication Engineering, University of Dhaka, Dhaka, Bangladesh

Author2Md. Omar Faruk
e-mail: umar.edu@gmail.com
Address: Atish Dipankar University of Science & Technology, Dhaka, Bangladesh

Author 3 Shahida Rafique
e-mail:srafique@du.ac.bd
Address:Dept. of Applied Physics, Electronics & Communication Engineering, University of Dhaka, Dhaka, bangladesh

*Corresponding author
e-mail: hasan.apece06@gmail.com
Tel: +8801920214900

This work is highly motivated by the continued interest on metallic nanowires. Recently there has been a great interest in the design, optimization, and fabrication of plasmonics-active metallic nanostructures since they provide a potential solution to key components in future high-capacity electronic and photonic circuits by providing spatial confinement of the light well beyond the diffraction limit. However, there have been various attempts in the past to understand different optical and electrical properties of different metallic nanowires. Properties such as Surface Plasmon Polariton Resonance and Scattering and Absorption Cross-sections of Silver and Gold nanowires are explored here in this work. Also the effect of diameter change on these cross-sections have been determined and analyzed.

Surface plasmon polaritons (SPPs) are electromagnetic waves that are strongly coupled to electron plasma oscillations at a metal – dielectric interface (Fig.1).

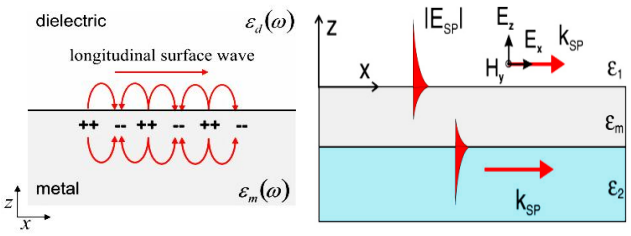

Fig.1. SPPpropagation along metal-dielectric interface

The SPP field is generally expressed as

$$\boldsymbol{E}_{SP} = \boldsymbol{E}_0^{\pm} e^{i(k_x x \pm k_z z - \omega t)} \quad (1)$$

Moreover, SPPs are strongly bound to the metal surface, leading to high lateral confinement and, thus, allows photonic manipulation below the diffraction limit.

Scattering cross-section expresses the amount of power scattered by the nanowire structure relative to the incident electromagnetic wave intensity while Absorption cross-section measures the amount of power absorbed by the nanowire structure relative to the incident electromagnetic wave intensity. These two cross-sections are expressed as (2) and (3) respectively.

$$\sigma_{scat}(\omega) = \frac{P_{scat}(\omega)}{I_{inc}(\omega)} \quad (2)$$

$$\sigma_{abs}(\omega) = \frac{P_{abs}(\omega)}{I_{inc}(\omega)} \quad (3)$$

where P_{scat} is the total scattered power, P_{abs} is the total power absorbed by the structure and I_{inc} is the incident intensity.

Researchers have used different approaches to study the properties of nanowires of several materials. In this work, Finite Difference Time Domain (FDTD) method has been employed.

II. Nanowire Literature Review

Generally, metallic NWs are synthesized by two methods: template-directed approaches [1-4] and chemical synthesis [5-9]. The plasmons supported by the metallic nanowires fabricated by templates usually suffer large losses due to scattering from the grain boundaries and rough surfaces of NWs [10]. On the other hand, chemical synthesis has been demonstrated as a simple and inexpensive route for the bottom-up preparation of metallic NWs with very smooth surfaces and without grain boundaries [5-9].

Au NWs have attracted considerable interests because of their high aspect ratios, unusual physical properties and potential applications in nanoelectronics, photonics and sensors. The large anisotropy of Au NWs and their subsequent assembly ability make them especially important building blocks for the linkage of nanoscale electronics and molecular devices. Many standard approaches have been extensively developed to produce Au NWs with desired shapes on the basis of particle assembly [11], surfactant radiation [8,12], template assistance [13]or physical deposition[14].

However, most of these early reported techniques usually resulted in the production of polycrystalline or relatively large diameter (45 nm) nanowires with poor morphology and rough surfaces. The most recent reports by Xia [15], Yang [16] and others [7, 17-18] delineated the synthesis of ultrathin Au NWs (less than 5 nm) by using oleylamine (OA) or combined chemicals as both 1-D growth templates and reducing agents.

The local electric field intensity for various metal nanostructures has been theoretically evaluated on the basis of the finite element method with

volume-integral equations [19-20] and also been theoretically evaluated by the FDTD method. Enhanced transmission peaks and sharp transmission dips are clearly observed around the theoretically SPP resonance frequencies [24]. Local field enhancements of 4.2×104 at 450 nm and 1.29×104 at 400 nm were obtained by the FDTD method at the center between the Ag particle and substrate when an Ag sphere with 10 nm radius was placed above the Ag flat substrate with a gap size of 0.5 nm and a plane wave was incident with an angle of 45°compared to the values of 4.2×104 at 450 nm and 1.3×104 at 410 nm obtained by analytical solutions [21]. Surface plasmon propagation along a nanowire can be straightforwardly demonstrated by local optical excitation [22]. For Ag NW with a diameter of 120 nm, the surface plasmon wavelength is 414 nm, which is considerably shorter than the exciting light wavelength of 785 nm. The ratio of these two wavelengths shows that the surface plasmon mode cannot directly couple to far field light neither in air nor in the glass substrate [10]. This finding implies that plasmon propagation along the wire is not radiation damped. However, chemically prepared Ag NWs with a well-developed crystal and surface structure sustain nonradiating surface plasmon modes with wavelengths shortened to about half the value of the exciting light [10].

The spectrum of plasmon resonances for metallic nanowires with a non–regular cross section in the 20–50 nm range also was investigated numerically [23]. At the resonance, dramatic field enhancement was observed at the vicinity of non–regular particles, where the field amplitude can reach several hundred times that of the illumination field [23].

Again, the propagation of SPPs in single crystalline Ag nanostructure was demonstrated and observed in the visible spectral region [25]. Propagation modes and single-guiding-mode conditions of Ag NW based SPP waveguides versus the operating wavelength (500-2000 nm) was also investigated and it was found that for wavelengths shorter than 615 nm, there is no cutoffradius for the guiding modes due tothe appearance of the interface modes and thus the single-guiding-mode operation is always satisfied [26]. Another interesting finding in the field of Plasmonic nanowires is that surface plasmons can be easily tuned by changing the surrounding dielectric materials, i.e., an extremely large tunability of surface plasmons on Ag NWs has been reported [27]. Using advanced fabrication techniques, nanowires can be utilized to produce switches [28] and efficient chemical and biological sensing systems [29].

III. Modeling and Design

A. Material model

A material model is automatically calculated based on the experimental refractive index data over the source bandwidth, as shown in Fig. 2.

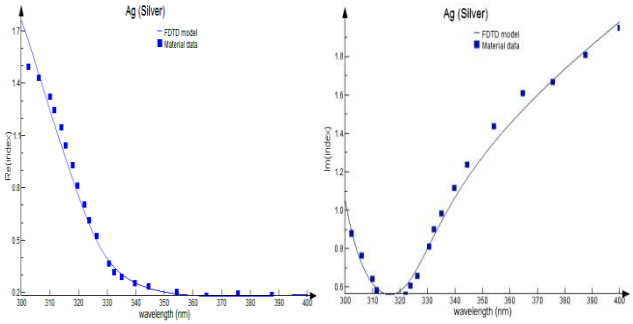

Fig. 2. Material data plot (Index)

The material fit, named FDTD model in the legend, can be adjusted by changing the Max coefficients and Tolerance parameters in the Material Explorer.

B. Source

TFSF (Total-Field Scattered-Field) sources are type of plane wave source, mostly used to particle scattering. The spectrum is as shown in Fig. 3 and modeled characteristic parameters are shown in TABLE 1.

TABLE 1. Modeled Source Parameters

Name	Type/Value
Injection axis	y-axis
Wavelength start	300 nm
Wavelength stop	400 nm
Polarization angle	0 degree

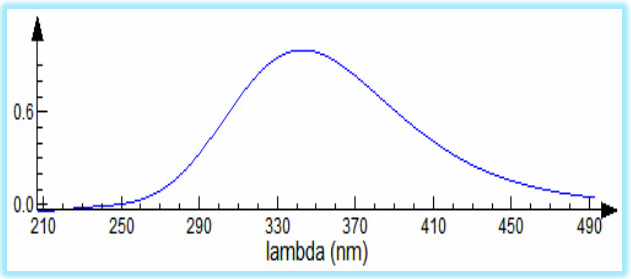

Fig. 3. Spectrum of the TFSF source

C. *Simulation Parameters*

Various parameters are as shown in TABLE 2 to TABLE 6 as considered for the simulation.

TABLE 2. *Mesh Parameters*

Name		Value (nm)
Override x mesh (dx)		0.5
Override y mesh(dy)		0.5
Geometry of the mesh	x (span)	110
	y (span)	110

TABLE 3. Time Monitor Set Up

Name	Type/Value
Monitor type	Point
Minimum sampling per cycle	10
Sampling rate	17843.9 THz
Monitor start time	0 fs
Monitor stop time	100 fs

TABLE 4. Total Analysis Group Set Up

Name		Value (nm)
Origin	x	0
	y	0
	z	0
Geometry	x (span)	90
	y (span)	90
	z (span)	90

TABLE 5. Scattering Analysis Group set up

Name		Value (nm)
Origin	x	0
	y	0
	z	0
Geometry	x (span)	110
	y (span)	110
	z (span)	110

TABLE 6. Simulation Set Up

Name		Type/Value
Simulation type		2D FDTD
Background Index		1.0
Simulation Time		100 fs
Simulation Areageometry	x (span)	800 nm
	y (span)	800 nm
Boundary conditions	x min	PML
	x max	PML
	y min	PML
	y max	PML
	No. of PML layers	12

Once the simulation has been set up, it will look as in the Fig.4.The nanowire is the circle in the center of the simulation region. There are two yellow boxes of monitors which surround the nanowire. In between the two monitor boxes is a third box drawn with of grey lines. This box shows the Total-field scattered-field (TFSF) source. The pink arrow shows the direction of propagation (k vector), and the blue arrow shows the polarization (E field vector).In the region inside the grey box, the total fields (incident plane wave field + any fields scattered by particle) are calculated.

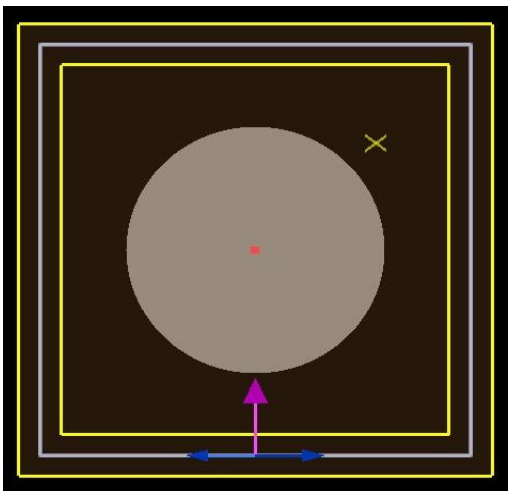

Fig. 4. Simulation Area showing the source and Mesh region

At the boundary of the source, the incident plane wave fields are subtracted, leaving only fields scattered by the particle inside the source.

IV. RESULTS AND DISCUSSION

A. Scattering and absorption cross-sections

Fig. 5 and Fig. 6 show the scattering and absorption cross-sections for Ag and Au NWs respectively with a radius of 35 nm.

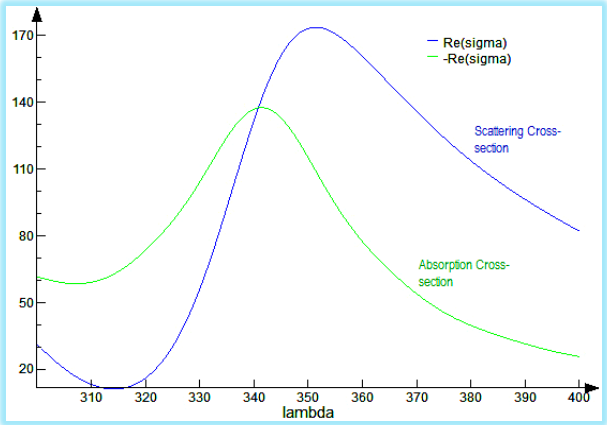

Fig. 5. Scattering and absorption cross-sections for r=35 nm of Ag NW

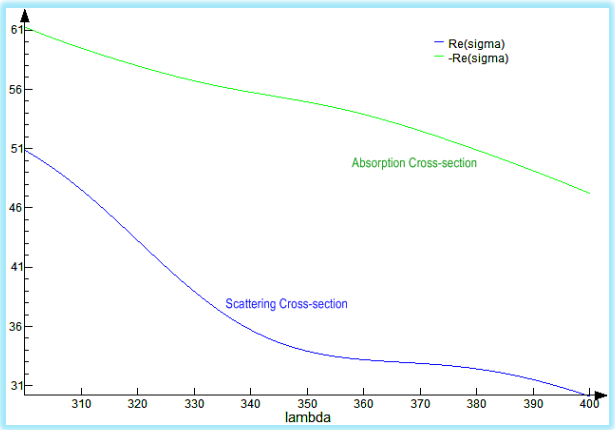

Fig. 6. Scattering and absorption cross-sections for r=35 nm of Au NW

There is hardly any resonance peak in case of Au NW as shown in Fig. 6.On the other hand, scattering cross section shows a peak at 350 nm while the absorption cross-section shows peak at around 342 nm in case of Ag NW.The peak arises from the LSP excitation.

Fig. 7 and Fig. 8 show the scattering and absorption cross-sections for Ag and Au NWs respectively with a radius of 30 nm.

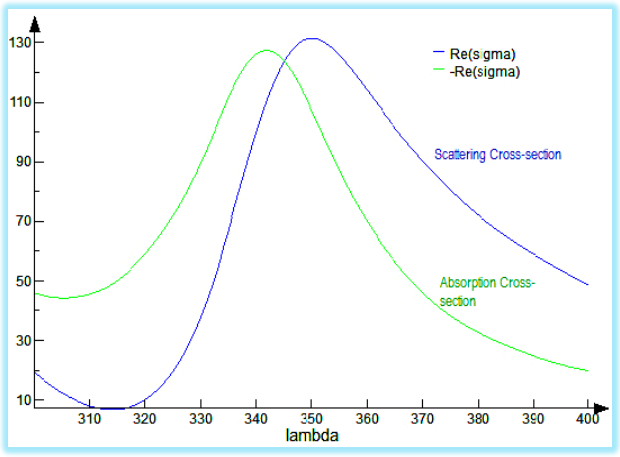

Fig. 7. Scattering and absorption cross-sections for r=30 nm of Ag NW

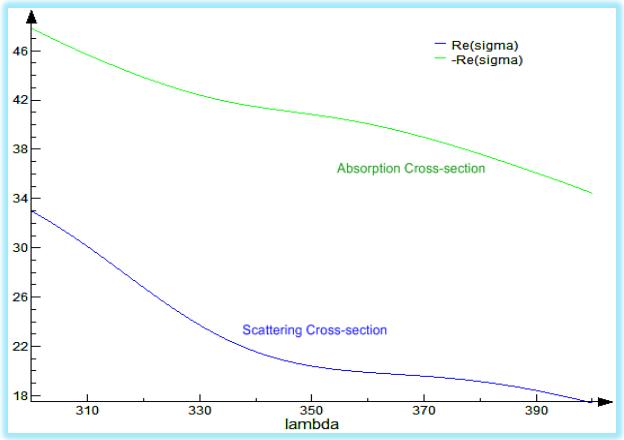

Fig. 8. Scattering and absorption cross-sections for r=30 nm of Au NW

Still there is no peak in case of Au NW while for Ag NW the scattering cross-section shows a sharp decrease in its peak value and this peak value approaches the value of absorption peak with the reduction in radius to 30 nm.

Fig. 9 and Fig. 10 show the scattering and absorption cross-sections for a radius of 25 nm of Ag and Au NWS respectively. Scattering cross section of Ag NW shows a peak at a value lower than 350 nm (for r=30 nm) while the absorption cross-section shows peak at around 342 nm irrespective of the reduction in radius, and also scattering cross-section value gets reduced to lower value than the absorption cross-section.

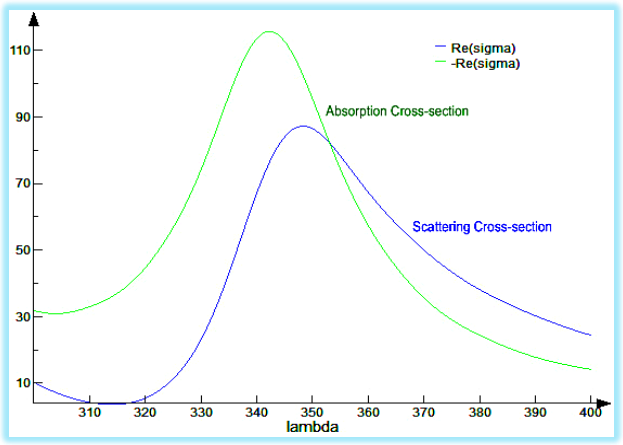

Fig. 9. Scattering and absorption cross-sections for r=25 nm of Ag NW

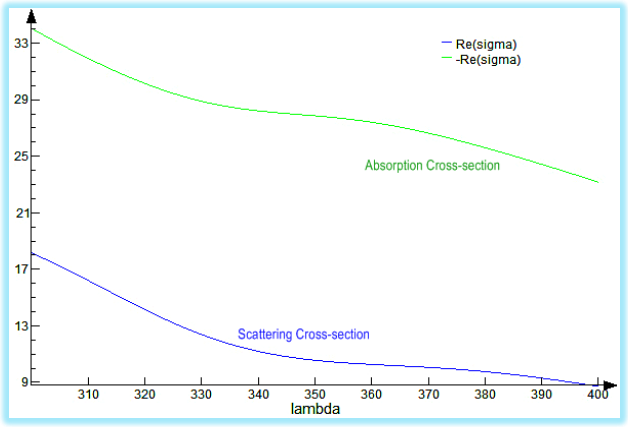

Fig. 10. Scattering and absorption cross-sections for r=25 nm of Au NW

From Fig. 11, it is clearly visible that further reduction in the radius of Ag NW causes zero shift to the absorption cross-section peak (the peak still occurs at around 342 nm) while the peak for scattering cross-section shifts to further lower value, a value lower than that for r= 20 nm.

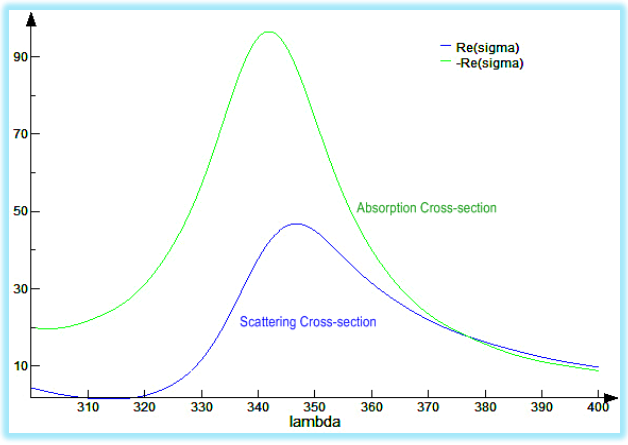

Fig. 11. Scattering and absorption cross-sections for r=20 nm of Ag NW

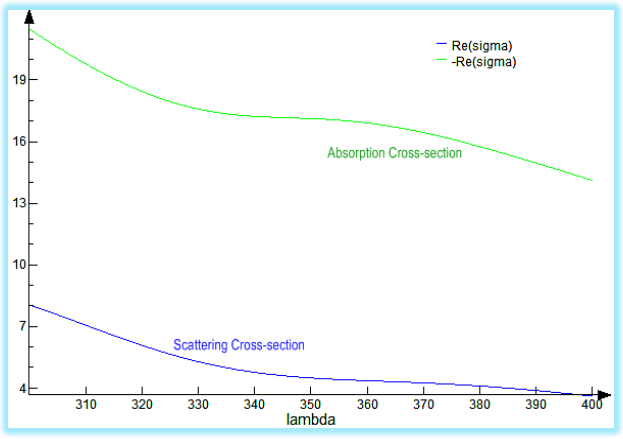

Fig. 12. Scattering and absorption cross-sections for r=20 nm of Au NW

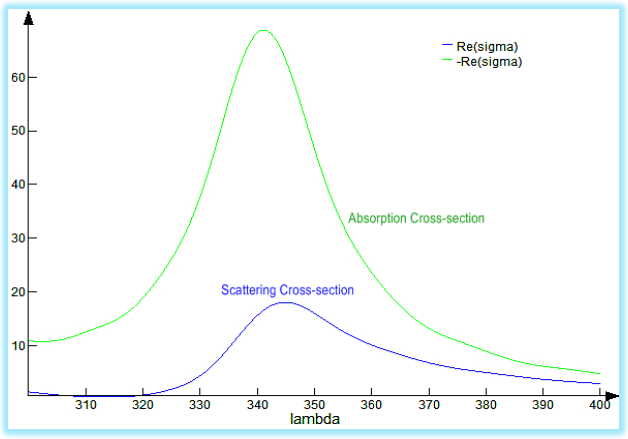

Fig. 13. Scattering and absorption cross-sections for r=15 nm of Ag NW

As indicated in Fig. 13, there is no significant change in the wavelength of resonance peak for absorption cross-section even when the Ag NW radius is reduced to 15 nm. The scattering cross-section peak in this case occurs at a further lower value of wavelength and also the amount of both the cross-sections is reduced with reduction in radius.

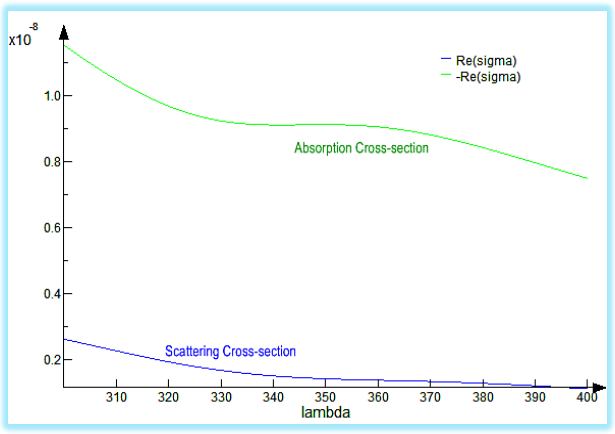

Fig. 14. Scattering and absorption cross-sections for r=15 nm of Au NW

Fig. 15 depicts the overall effect of radius change on the Scattering cross-section value for Ag NW. As shown in the figure, the scattering cross-section peak shifts to lower wavelength value with the decrease in radius of the nanowire. Also the magnitude of the cross-section decreases with decrease in radius. The plot is made by measuring the scattering cross-sections for r= 28, 27, 26, 25, 24 nm.

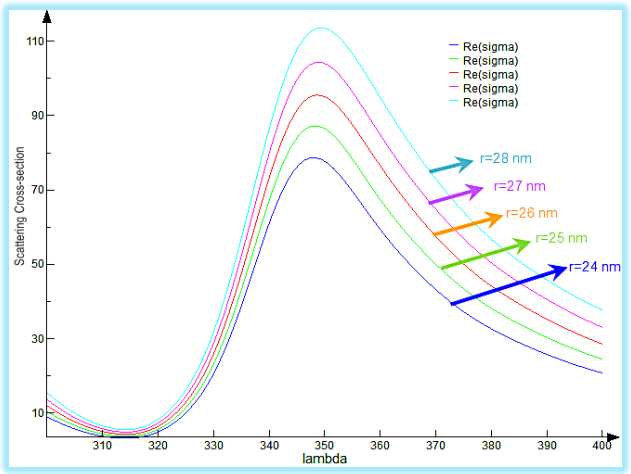

Fig. 15. Change in scattering cross-sections with radius of Ag NW

Fig. 16 illustrates the effect of radius change on the absorption cross-section value of Ag NW. The scattering cross-section peak doesn't shift significantly to lower wavelength value with the decrease in radius of the nanowire, but the magnitude of the cross-section decreases with decrease in r.

Fig. 16 is also plotted by measuring the scattering cross-sections for r= 28, 27, 26, 25, 24 nm.

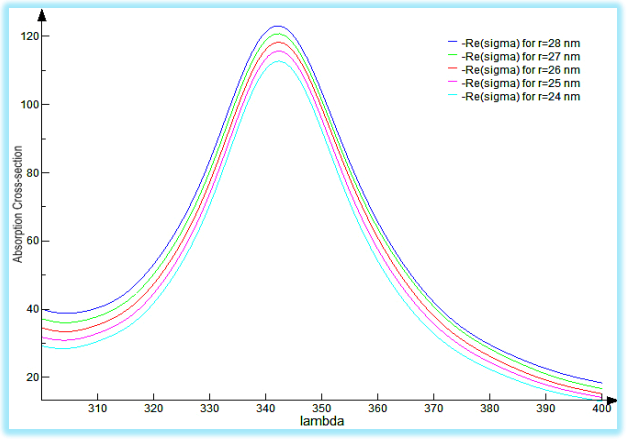

Fig. 16. Change in absorption cross-sections with radius of Ag NW

Fig. 17 shows that increasing radius results in upward shift to the cross-sections in case of Au NW, but without any sharp peak.

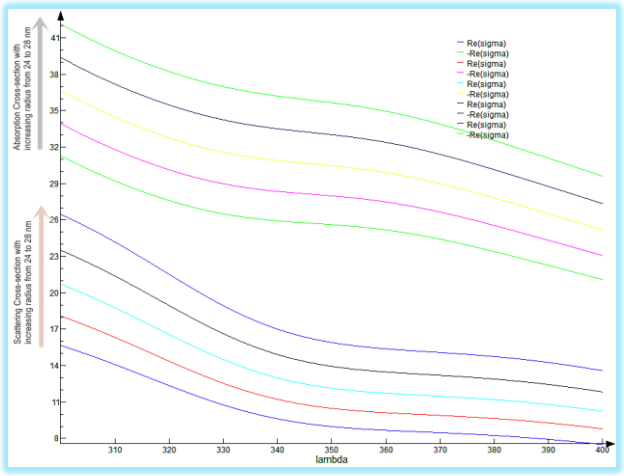

Fig. 17. Change in Scattering and absorption cross-sections with radius of Au NW

B. Local Electric Field Intensity

The electric field maximum is determined by the local structure and the LSP resonance at the particular site, e.g., the enhancement is confined within a few nanometers from the edge, although these are not completely distinguished. The sharp decay of the local field maximum is clearly explained by the peak shift of the LSP resonance to shorter wavelength and by the decreased coupling with increasing the spacing.

Fig. 18 shows the electric field intensity distribution when radius of the nanowire structure is 30 nm. The SPP resonance is slightly sharper for Ag NW than Au NW when radius is set to 30 nm.

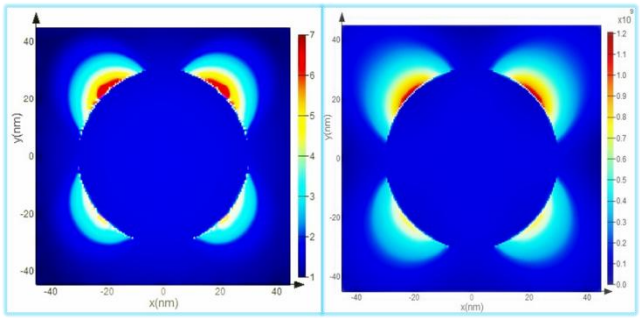

(a) (b)

Fig. 18. Intensity of electric field E_y calculated with a 0.5 nm mesh when r=30 nm of (a) Ag NW, (b) Au NW

However, the difference in resonances is prominently clear from Fig. 19 and Fig. 20 in

which case the radius is set to 25 and 20 nm for both NW structures respectively. These figures actually show a distribution of $|E_y|^2$. However, the electric field is highly intense when r= 25 nm.

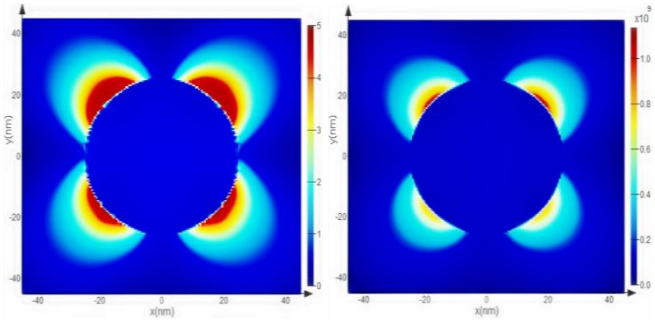

(a) (b)

Fig. 19. Intensity of electric field E_y calculated with a 0.5nm mesh when r=25 nm of (a) Ag NW, (b) Au NW

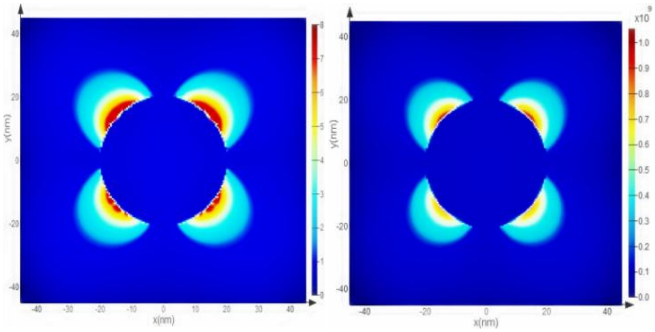

(a) (b)

Fig. 20. Intensity of electric field E_y calculated with a 0.5 nm mesh when r=20 nm of (a) Ag NW, (b) Au NW

Fig. 21illustrates one of the most interesting findings; when the radius is reduced to 15 nm, the electric field intensity at the Au-Air interface is much stronger than that of Ag-Air interface. Therefore, Au NW can support strong SPR at a diameter lower than the Ag NW which is utilized in many applications.

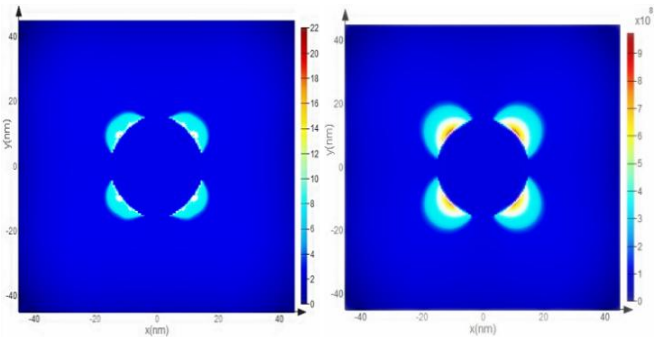

(a) (b)

Fig. 21. Intensity of electric field E_y calculated with a 0.5 nm mesh when r=15 nm of (a) Ag NW, (b) Au NW

V. Conclusion

The analysis of Plasmonic nanowires using Finite Difference Time Domain (FDTD) method is successfully completed and presented here. It is concluded that the nanowire structures of various metals like Silver and Gold can be modeled and analyzed using Finite Difference Time Domain method to determine and observe the surface plasmon polariton resonance and also absorption and scattering cross-sections. It is found that different properties of nanowire change with a change in its dimension. And it is also realized that silver nanowire has excellent absorption and scattering cross-section spectra with sharp peaks and excellent surface plasmon polariton resonance. In contrast, Gold nanowire shows better surface plasmon resonance characteristics in various dimensions and even at 15 nm radius.

However, the nanowire structure modeled here is of circular cross-section. Some other structures, such as elliptical, hexagonal etc., may be investigated to study the change in characteristics of the nanowire network. Investigation on some other non-regular cross-sections is a future target.

In our designed model of the nanowire structure, air has been chosen as the background material, i.e., metal-air interface provides the required interface for the surface plasmon resonance to occur at the interface. To investigate the nanowire structures with some other background materials, e.g., SiO_2, is another future option.

Again, several available methods could also have been tried other than FDTD. But FDTD method is very simple and easy to understand and also provides better fit with experiment in most cases reported so far. That is why the FDTD technique has been considered here in this work.

References

[1] D. Ugarte, A. Chatelain, and W. A. de Heer, “Nanocapillarity and Chemistry in Carbon Nanotubes”, Science 274(5294), pp.1897–1899 (1996).

[2] E. Braun, Y. Eichen, U. Sivan, and G. Ben-Yoseph, "DNA-templated assembly and electrode attachment of a conducting silver wire", Nature 391(6669), pp.775–778 (1998).

[3] T. D. Lazzara, G. R. Bourret, R. B. Lennox, and T. G. M. van de Ven, "Polymer Templated Synthesis of AgCN and Ag nanowires", Chem. Materials 21(10), pp.2020–2026 (2009).

[4] R. L. Zong, J. Zhou, Q. Li, B. Du, B. Li, M. Fu, X. W. Qi, L. T. Li, and S. Buddhudu, "Synthesis and Optical Properties of Silver Nanowire Arrays Embedded in Anodic Alumina Membrane",J. Phys. Chem. B 108(43), pp.16713–16716 (2004).

[5] Y. G. Sun, B. Mayers, T. Herricks, and Y. N. Xia, "Polyol Synthesis of Uniform Silver Nanowires: A Plausible Growth Mechanism and the Supporting Evidence",NanoLett. 3(7), pp.955–960 (2003).

[6] K. E. Korte, S. E. Skrabalak, and Y. N. Xia, "Rapid synthesis of silver nanowires through a CuCl- or $CuCl_2$-mediated polyol process",J. Mater. Chem. 18(4), pp.437–441 (2008).

[7] C. Wang, Y. J. Hu, C. M. Lieber, and S. H. Sun, "Ultrathin Au nanowires and their transport properties", J. Am. Chem. Soc. 130(28), pp.8902–8903 (2008).

[8] F. Kim, K. Sohn, J. S. Wu, and J. X. Huang, "Chemical synthesis of gold nanowires in acidic solutions", J. Am. Chem. Soc. 130(44), pp.14442–14443(2008).

[9] X. X. Li, L. Wang, and G. Q. Yan,"Review: recent research progress on preparation of silver nanowires by soft solution methods and their applications",Cryst. Res. Technol. 46(5), pp.427–438 (2011).

[10] H. Ditlbacher, A. Hohenau, D. Wagner, U. Kreibig, M. Rogers, F. Hofer, F. R. Aussenegg, and J. R. Krenn, "Silver nanowires as surface plasmon resonators", Phys. Rev. Lett. 95(25), pp.257403.1-4 (2005).

[11] L. H. Pei, K. Mori, and M. Adachi, "Formation process of two-dimensional networked gold nanowires by citrate reduction of $AuCl_4^-$ and the shape stabilization", Langmuir 20(18), pp.7837-7843 (2004).

[12] X. G. Liu, N. Q. Wu, B. H. Wunsch, R. J. Barsotti, and F. Stellacci, "Shape-controlled Growth of Micrometer-sized Gold Crystals by a Slow Reduction Method", Small, 2, pp.1046-1050 (2006).

[13] (a) H. Bai, K. Xu, Y. Xu, and H. Matsui, "Fabrication of Au Nanowires of Uniform Length and Diameter using a Monodisperse and Rigid Biomolecular Template: Collagen-like Tripple Helix",Angew. Chem. Intl. Ed. 46(18), pp.3319-3322 (2007); (b) P. Forrer, F. Schlottig, H. Siegenthaler, and M. Textor, "Electrochemical Preparation and Surface Properties of Gold Nanowire Arrays Formed by the Template Technique", J. Appl. Electrochem. 30(5), pp.533-541 (2000).

[14] C. E. Cross, J. C. Hemminger, and R. M. Penner, "Physical vapor deposition of one-dimensional nanoparticle arrays on graphite: Seeding the Electrodeposition of gold nanowires", Langmuir 23(20), pp.10372-10379 (2007).

[15] (a) X. M. Lu, M. S. Yavuz, H. Y. Tuan, B. A. Korgel, and Y. N. Xia, J. Am. Chem. Soc. 130(28), pp. 8900-8901 (2008); (b) Z. Li, J. Tao, X. M. Lu, Y. Zhu and Y. N. Xia, "Facile synthesis of ultrathin Au nanorods by aging the AuCl (oleylamine) complex with amorphous Fe nanoparticles in chloroform", Nano. Lett. 8(9), pp.3052-3055 (2008).

[16] Z. Huo, C. K. Tsung, W. Huang, X. Zhang and P. Yang, "Sub-two nanometer single crystal Au nanowires", NanoLett. 8(7), pp.2041-2044 (2008).

[17] A. Halder and N. Ravishankar, "Ultrafine Single-Crystalline Gold Nanowire Arrays by Oriented Attachment", Advanced Materials 19(14), pp.1854-1858 (2007).

[18] N. Pazos-Pe´rez, D. Baranov, S. Irsen, M. Hilgendorff, L. M. Liz-Marza´n and M. Giersig, "Synthesis of flexible, ultrathin gold nanowires in organic media", Langmuir 24(17), pp.9855-9860 (2008).

[19] J. P. Kottmann, O. J. F. Martin, D. R. Smith, S. Schultz, "Dramatic localized electromagnetic enhancement in plasmon resonant nanowires", Chem. Phys. Lett. 341, pp.1-6 (2001).

[20] J. P. Kottmann, O. J. F. Martin, D. R. Smith, S. Schultz, "Plasmon resonances of silver nanowires with a non-regular cross-section", Phys. Rev. B64(23), pp. 235402.1-10 (2001).

[21] M. Futamata , Y. Maruyama, and M. Ishikawa, "Local electric field and scattering cross section of Ag nanoparticles under surface plasmon resonance by finite difference time domain method", J. Phys. Chem. B 107(31), pp. 7607 – 7617 (2003).

[22] R. M. Dickson and L. A. Lyon, "Unidirectional plasmon propagation in metallic nanowires", J. Phys. Chem. B 104(26), pp.6095-6098 (2000).

[23] O. J. F. Martin, "Plasmon Resonances in Nanowires with a Non-regular Cross-Section", Springer, Topics in Appl. Phys. 88, pp. 183-210 (2003).

[24] M. W. Kim, T. T. Kim, J. E. Kim and H. Y. Park, "Surface plasmon polariton resonance and transmission enhancement of light through subwavelength slit arrays in metallic films", Opt. Express 17(15),pp. 12315-12322 (2009).

[25] S. Kumar, Y.W. Lu, A. Huck and U. L. Andersen, "Propagation of plasmons in designed single crystalline silver nanostructures", Opt. Express 20(22), pp.24614-24622 (2012).

[26] Q. Li, and M. Qiu, "Plasmonic wave propagation in silver nanowires: guiding modes or not?"Opt. Express 21(7), pp. 8587-8595 (2013).

[27] H. Wei, S. Zhang, X. Tian, and H. Xu, "Highly tunable propagating surface plasmons on supported silver nanowires", PNAS110(12), pp. 4494-4499 (2013).

[28] T. Nikolajsen and K. Leosson, S. I. Bozhevolnyi, "Surface plasmonpolariton based modulators and switches operating at telecom wavelengths" Appl. Phys. Lett. 85(24), pp.5833-5835 (2004).

[29] T. Vo-Dinh, A. Dhawan, S. J. Norton, C. G. Khoury, Hsin-Neng Wang, V. Misra, and Michael D. Gerhold, "Plasmonic nanoparticles and nanowires: design, fabrication and application in sensing",J. Phys. Chem. C 114, pp.7480–7488 (2010).

[30] FDTD solutions 8.5, Lumerical Inc. (2012).